VERSITA

Cent. Eur. J. Chem. • 9(3) • 2011 • 460-465
DOI: 10.2478/s11532-011-0027-5

Central European Journal of **Chemistry**

Influence of heat treatment on the phase transition of $ZrMo_2O_8$ and photocatalytic activity

Research Article

Maria N. Mancheva*[,1], Reni S. Iordanova[1], Yanko B. Dimitriev[2], Georgi G.Tyuliev[3], Tzvetoslav Ch. Iliev[4]

[1]*Institute of General and Inorganic Chemistry, Bulgarian Academy of Science, Sofia 1113, Bulgaria*

[2]*University of Chemical Technology and Metallurgy, Sofia 1756, Bulgaria*

[3]*Institute of Catalysis, Bulgarian Academy of Science, Sofia 1113, Bulgaria*

[4]*Geological Institute, Bulgarian Academy of Science, Sofia 1113, Bulgaria*

Received 19 October 2010; Accepted 8 February 2011

Abstract: $ZrMo_2O_7(OH)_2 \cdot 2H_2O$ was obtained from $ZrOCl_2 \cdot 2H_2O$ and $Na_2MoO_4 \cdot 2H_2O$ by a coprecipitation method. The phase and structural changes occurred during the heat-treatment of $ZrMo_2O_7(OH)_2 \cdot 2H_2O$ were investigated by XRD, IR and XPS analysis. The sequence of phase transformation can be divided into three stages: (1) transformation of $ZrMo_2O_7(OH)_2 \cdot 2H_2O$ to orthorhombic LT-$ZrMo_2O_8$ up to 300°C; (2) obtaining of mixture of both polymorphs of $ZrMo_2O_8$: cubic and trigonal at 400°C; (3) conversion to single trigonal (α) $ZrMo_2O_8$ above 450°C. The microstructure of the obtained trigonal (α) $ZrMo_2O_8$ was observed by scanning electron microscopy (SEM). The particle sizes were below 0.5 μm. The specific surface area was measured by modified BET method. The photocatalytic activity of the obtained trigonal (α) $ZrMo_2O_8$ powders was investigated by degradation of a model aqueous solution of Malachite Green (MG) upon UV-light irradiation.

Keywords: *$ZrMo_2O_8$ • Nanoparticles • Phase transformation • Photocatalytic activity*

© *Versita Sp. z o.o.*

1. Introduction

The investigations of the $ZrMo_2O_8$ have been connected with synthesis, structures and phase transitions at different temperatures and pressures [1-11]. Some physical properties such as zero or negative thermal expansion (NTE) coefficient are also investigated [7-10]. On the other hand the $ZrMo_2O_8$ exhibits luminescence properties [12], catalytic properties: selective oxidation of dimethyl ether to formaldehyde [13] and oxidative dehydrogenation of propene [14]. Sahoo *et al.* [15,16] shown that the $ZrMo_2O_8$ possesses a photocatalytic activity at degradation of various dyes under UV-light irradiation. Photocatalytic degradation of organic contaminants in water by different inorganic materials (TiO_2, ZnO, $ZnWO_4$, Bi_2MoO_6 and *etc.*) is one of the most attractive areas in recent years [17-20].

$ZrMo_2O_8$ has several polymorphs: monoclinic (β), trigonal (α), cubic, orthorhombic LT and high pressure phases (monoclinic (δ) and triclinic (ε)) [1-11]. The different polymorph modifications can be obtained by selecting appropriate synthesis method. The thermodynamically stable polymorphs are the monoclinic (β) and trigonal (α) $ZrMo_2O_8$ [1-3]. These phases were prepared by a conventional solid-state reaction or dehydration of $ZrMo_2O_7(OH)_2 \cdot 2H_2O$ above 390°C [1-5,15,16]. The phase transformation from monoclinic (β) to trigonal (α) $ZrMo_2O_8$ was observed at 690°C [2]. Under influence of pressure, the trigonal (α) $ZrMo_2O_8$ was converted to monoclinic (δ) $ZrMo_2O_8$ (~1.06-1.11 GPa) which was further transformed to triclinic (ε) $ZrMo_2O_8$ (~2.5GPa) [3-6]. The orthorhombic LT-$ZrMo_2O_8$ was obtained by dehydration of $ZrMo_2O_7(OH)_2 \cdot 2H_2O$ at 300°C for 8 h and above this temperature it was transformed into cubic $ZrMo_2O_8$ [11]. The thermodynamically metastable cubic $ZrMo_2O_8$ was obtained by controlled dehydration of $ZrMo_2O_7(OH)_2 \cdot 2H_2O$ and by a non-hydrolytic sol-gel method [7-10]. The cubic $ZrMo_2O_8$ was converted to trigonal (α) $ZrMo_2O_8$ at 390°C [7]. From the above analysis it is clear that the cubic and orthorhombic LT-$ZrMo_2O_8$ were prepared only by a coprecipitation method or non-hydrolytic sol-gel method [7-11].

* *E-mail: mancheva@svr.igic.bas.bg*

In the literature, there is no enough data about phase transformation depending on time and temperature. In our previous paper, we synthesised the monoclinic (β) and the trigonal (α) $ZrMo_2O_8$ phases by three different methods: solid state reaction, melt quenching method, and mechanochemically assisted solid state synthesis [21]. It was established that the flow-card of heat-treatment essentially influence on the mechanism of the phase transformation and the type of the final products. The present study is a continuation in this direction. We choose the coprecipitation method in order to investigate the phase and structural transformation of $ZrMo_2O_7(OH)_2$•2(H_2O) as a function of heat-treatment. Additionally, the photocatalytic properties of the obtained product are evaluated by examining the degradation of Malachite Green (MG) upon UV-light irradiation.

2. Experimental Procedure

The precursor $ZrMo_2O_7(OH)_2$•$2H_2O$ was prepared according to Clearfield and Blessing whose used the coprecipitation method [22]. Aqueous solutions of the reactants, 25 mL 0.5 *M* $ZrOCl_2$•$2H_2O$ (Aldrich, 99.99%) and 25 mL 1 *M* Na_2MoO_4•$2H_2O$ (Sigma, 99.99%), were mixed by simultaneous dropwise addition to 10 mL water under continuous stirring. The obtained gel was aged for two days in the mother liquor. The gel and mother liquor were refluxed for 3 days. The solid obtained was washed with 1 *M* HCl to remove the sodium ion and then with H_2O to remove the chloride ion. In our experiments we examined the transformation of $ZrMo_2O_7(OH)_2$•$2H_2O$ by stepwise heating at 100, 200, 300, 400, 450 and 600°C in air for 3 h. The phases obtained and their transformations were monitored by x-ray diffraction (XRD), infrared (IR) spectroscopy and x-ray photoelectron spectroscopy (XPS). Powder XRD patterns of the samples were registered at room temperature with a Bruker D8 Advance diffractometer using Cu-K_α radiation. Infrared spectra of the samples were registered in the range 1200-400 cm^{-1} using the KBr pellet technique on a Nicolet-320 FTIR spectrometer with 64 scans and a resolution of ±1 cm^{-1}. The specific surface area of the samples was measured using a modified BET method. The XPS measurements were carried out in the UHV chamber of an ESCALAB-MkII (VG Scientific) electron spectrometer using MgK_α excitation with a total instrumental resolution of ~ 1 eV. Energy calibration was performed, taking the C1s line at 285 eV as a reference. The microstructure of the obtained sample was characterized by scanning electron microscopy (JOEL-SUPERROBE 733). The photocatalytic activity of the obtained $ZrMo_2O_8$ powder was evaluated by degradation of a model aqueous solution of Malachite Green (MG-Sigma-Aldrich) upon UV-light irradiation. The UV irradiation was carrying out by UV-lamp (Sulvania BLB, 18 W, λ ~ 315–400 nm). The aqueous solution of MG (150 mL, 5 ppm) containing 0.1 g of as-prepared powder was placed in a vessel. Before photodegradation, an adsorption-desorption equilibrium state was established by ultrasonic and mechanical stirring for 10 min. Volumes of 3 mL of solution were taken at given time interval and separated through centrifugation (5000 rpm, 5 min). Then the concentration of MG in the solution was analysed with a Jenway 6400 spectrophotometer.

3. Results and Discussion

Fig. 1 presents XRD patterns of the $ZrMo_2O_7(OH)_2$•2(H_2O) depending on the heating temperature. At 200°C a set of new broad peaks was observed, which correspond to orthorhombic LT-$ZrMo_2O_8$ phase (JCPDS-72-8226). This phase remains up to 300°C (Fig. 1c). The results are in good agreement with published data about the synthesis of orthorhombic LT-$ZrMo_2O_8$ phase applying coprecipitation method [8,11]. For comparison, by mechanochemical solid state synthesis up to 300°C only an amorphous phase and traces of the initial compounds were detected [21]. On Fig. 1d it is shown that at 400°C orthorhombic LT-$ZrMo_2O_8$ transforms into trigonal (α) $ZrMo_2O_8$ (JCPDS-79-0576) and cubic $ZrMo_2O_8$ phases (d=5.28Å, d=4.09Å, d=3.73Å) [7]. At this temperature the predominant phase was metastable cubic $ZrMo_2O_8$. Further increase of the temperature up to 450°C led to complete transformation of cubic into trigonal (α) $ZrMo_2O_8$ phase. Above this temperature the phase transformation was not observed and trigonal (α) $ZrMo_2O_8$ phase only exists. We made an additional heat-treatment at 600°C in order to check the process of densification of the material which was illustrated by SEM analysis (Fig. 3b). Phase transformation was not observed after this heat-treatment (Fig. 1f).

The phase and structural transformations of the $ZrMo_2O_7(OH)_2$•2(H_2O) during the heat-treatment were studied by IR spectroscopy. The structural data of the all polymorphs and the available vibrational spectra of monoclinic (β) and trigonal (α) $ZrMo_2O_8$ were used for identification of the samples prepared by us [1-3,7,11,21-27]. The structure of $ZrMo_2O_7(OH)_2$•2(H_2O) is built up of ZrO_6(OH)-pentagonal bipyramids and distorted MoO_4(OH)(H_2O)-octhahedra [22]. According to Allen *et al*. [11] the structural units building the orthorhombic LT- $ZrMo_2O_8$ are similar to the structural units building the trigonal (α) $ZrMo_2O_8$ (ZrO_6 octahedra and MoO_4 tetrahedra). The cubic $ZrMo_2O_8$ is isostructural with the

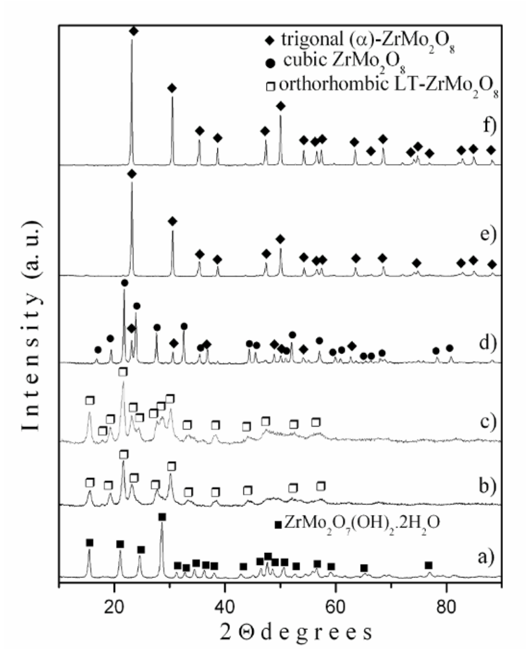

Figure 1. XRD patterns of the $ZrMo_2O_7(OH)_2{\bullet}2H_2O$ after heat-treatment at: a) 100°C; b) 200°C; c) 300°C; d) 400°C; e) 450°C; f) 600°C.

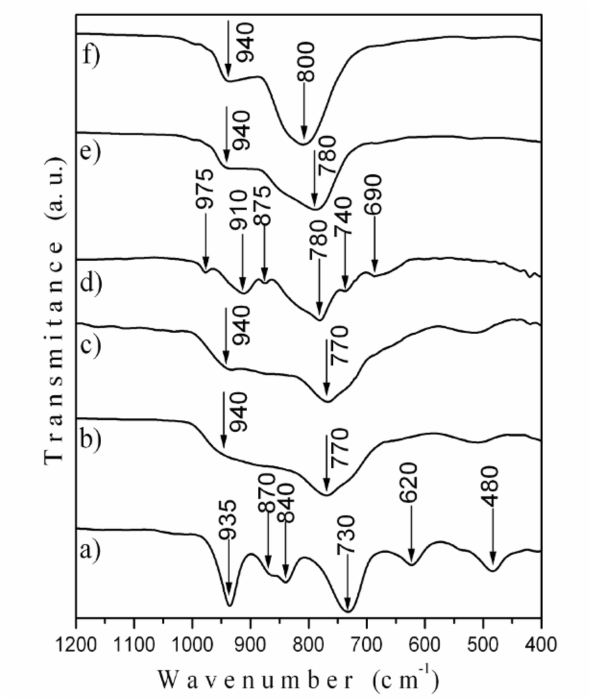

Figure 2. IR spectra of the $ZrMo_2O_7(OH)_2{\bullet}2H_2O$ after heat-treatment at: a) 100°C; b) 200°C; c) 300°C; d) 400°C; e) 450°C; f) 600°C.

cubic ZrW_2O_8 consists of corner-sharing ZrO_6 octahedra and two crystallographically distinct MoO_4 tetrahedra [7]. In the IR spectrum of the initial sample there are bands at 935, 870, 840, 730, 620 and 480 cm^{-1} which are typical for the $ZrMo_2O_7(OH)_2{\bullet}2(H_2O)$ (Fig. 2a) [22].

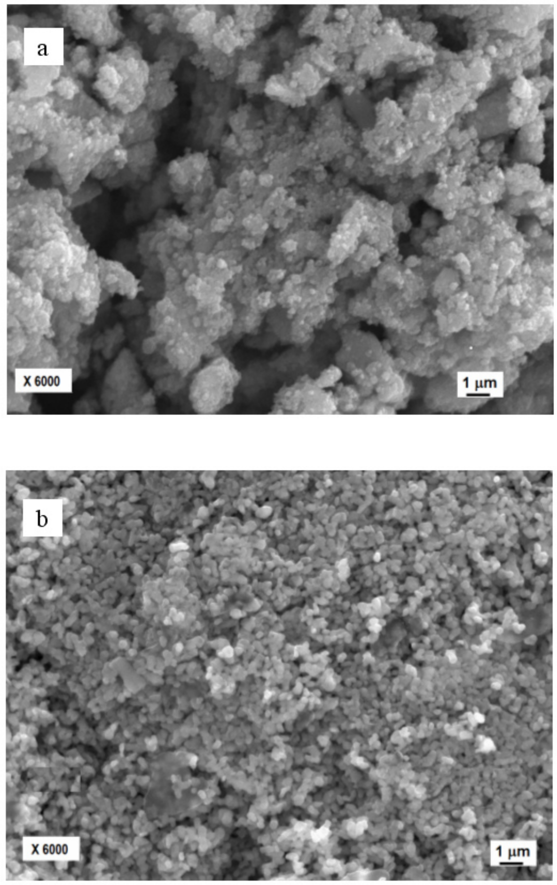

Figure 3. SEM image of the trigonal (α) $ZrMo_2O_8$ obtained after (a) heat-treated at 450°C, (b) additionally calcinated at 600°C.

The appearance of new broad bands centred at 940 and 770 cm^{-1} is connected with a change of the main structural units from $MoO_4(OH)(H_2O)$-octhahedra to MoO_4 tetrahedra (Fig. 2b and 2c). Taking into account the above structural data we attributed the band at 770 cm^{-1} to a triply degenerated v_3 asymmetric stretching mode of distorted MoO_4 units building the orthorhombic LT-$ZrMo_2O_8$ which was formed at 200°C. The high frequency band at 940 cm^{-1} is due to activation of the v_1 symmetric vibration of the same groups [11]. In the IR spectrum of sample heated at 400°C the number of absorption bands increased which can be attributed to phase transformation of orthorhombic LT-$ZrMo_2O_8$ to cubic $ZrMo_2O_8$,which was established by XRD analysis. The assignment of the characteristic bands of cubic $ZrMo_2O_8$ was made according to the vibrational spectra of cubic ZrW_2O_8 [25-27]. The bands at 975, 910 and 875 cm^{-1} can be assigned to symmetric v_1 stretching vibration of MoO_4 groups with low symmetry building cubic $ZrMo_2O_8$ and those at 780, 740 and 690 cm^{-1} can be attributed to asymmetric v_3 stretching modes of the same groups [25-27] (Fig. 2d). The phase transformation from cubic

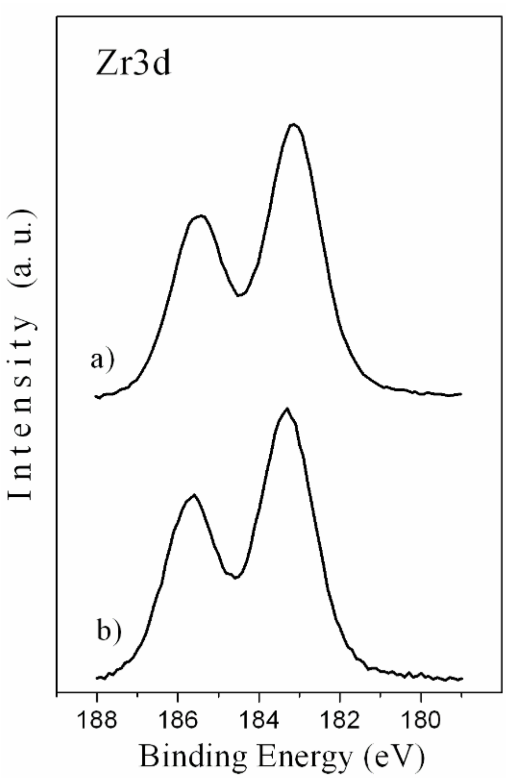

Figure 4. Binding energy of Zr3d peaks of: a) $ZrMo_2O_7(OH)_2$•$2H_2O$; b) trigonal (α) $ZrMo_2O_8$ obtained after heat-treated at 450°C.

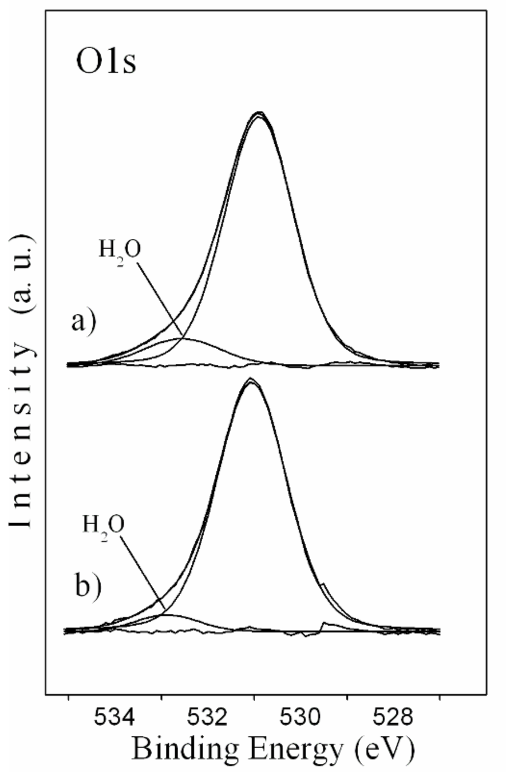

Figure 6. Binding energy of O1s peaks of: a) $ZrMo_2O_7(OH)_2$•$2H_2O$; b) trigonal (α) $ZrMo_2O_8$ obtained after heat-treated at 450°C.

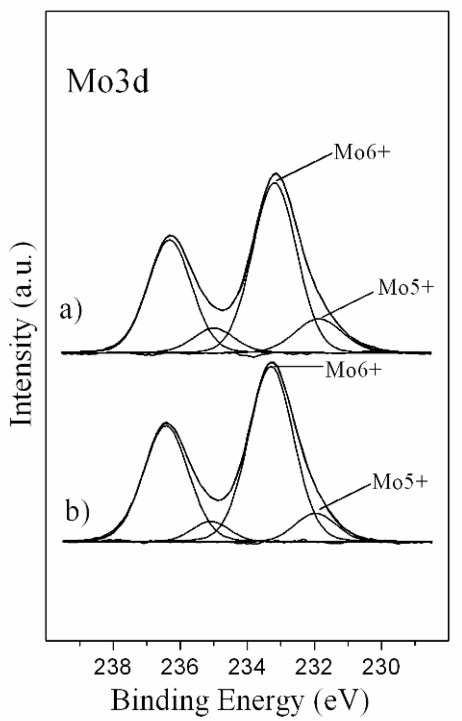

Figure 5. Binding energy of Mo3d peaks of: a) $ZrMo_2O_7(OH)_2$•$2H_2O$; b) trigonal (α) $ZrMo_2O_8$ obtained after heat-treated at 450°C.

to trigonal (α) $ZrMo_2O_8$ at 450°C was evidenced by the appearance of two bands at 940 and 780 cm^{-1} (Fig. 2e) [1,21,23]. The increase of temperature up to 600°C led to a shift of the band at 780 cm^{-1} to more symmetrical band centred at 800 cm^{-1}. This fact can be explained as a result of the formation of more regular MoO_4 tetrahedra with shorter Mo-O distances in the structure of trigonal (α) $ZrMo_2O_8$ heated at 600°C (Fig. 2f).

The microstructure of the $ZrMo_2O_8$ powders was investigated by SEM observations. It can be seen that $ZrMo_2O_8$ powders (Figs. 3a, 3b) consist of spherical submicron particles. Cavities and tendency to agglomeration were observed in the sample obtained at 450°C (Fig. 3a). Densification and initial stage of sintering of particles were occurred in the sample additionally calcinated at 600°C (Fig. 3b).

The specific surface area of the sample obtained at 450°C is 99 m^2 g^{-1} and decreases to 5.5 m^2 g^{-1} after heat-treatment at 600°C. The lower specific surface area is in good agreement to the observed densification at high temperature.

The XPS analysis gives information on the oxidation state of the Mo and Zr ions and the presence of H_2O in the precursor and the obtained product. Table 1 shows the value of the binding energy of the $Zr3d_{5/2}$, $Mo3d_{5/2}$

Table 1. The value of the binding energies of Zr3d, Mo3d and O1s in the samples (in eV) (the value in parentheses indicate the relative amount of different components)

Samples	$Zr3d_{5/2}$	$Mo3d_{5/2}$		O1s	
		LBE*	HBE**	LBE*	HBE**
$ZrMo_2O_7(OH)_2$•$2(H_2O)$	183.10	231.80 (18%)	233.15 (82%)	530.9 (90%)	532.6 (10%)
trigonal (α) $ZrMo_2O_8$	183.35	232.00 (13%)	233.30 (87%)	531.1 (95%)	532.9 (5%)

** - Lower Binding Energy component (LBE)*
*** - Higher Binding Energy component (HBE)*

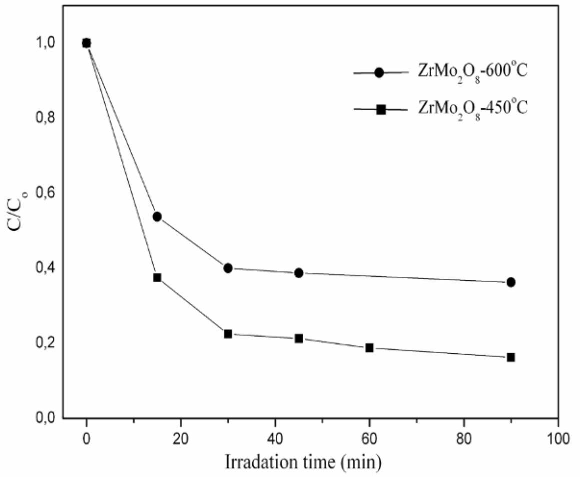

Figure 7. Photodecomposition of the MG during UV-light irradiation by $ZrMo_2O_8$ samples.

and O1s levels of both samples. Figs. 4, 5 and 6 present the XPS spectra of Zr3, Mo3d and O1s lines. The binding energy of the $Zr5d_{5/2}$ line is 183.10 eV and 183.35 eV in the $ZrMo_2O_7(OH)_2$•$2(H_2O)$ and trigonal (α) $ZrMo_2O_8$, respectively (Fig. 4). These values are typical of the Zr in 4+ oxidation state in mixed oxides which is in good agreement with published data [28-30]. The Mo3d levels were presented by two components with binding energies around 233.15 ÷ 233.30 eV (High Binding Energy) and at 231.80 ÷ 232.00 eV (Low Binding Energy) (Fig. 5). The value of a higher binding energy around 233.30 eV can be assigned to the Mo in 6+ oxidation state while the value of lower binding energy at 231.80 eV may be attributed to the Mo in 5+ oxidation state [31-33]. The amount of Mo in 5+ oxidative state in the precursor is 18 % and decreases to 13% in the trigonal (α) $ZrMo_2O_8$. The O1s levels were fitted into two peaks (Fig. 6). The main peak is centered at 530.9÷531.1 eV, which can be attributed to a binding energy of the O-atom between two neighborly polydehra in both structures [1-3,22]. The high energy shoulder at 532.6 eV can be ascribed to present of H_2O in the $ZrMo_2O_7(OH)_2$•$2(H_2O)$ [34,35]. The amount of the H_2O decreases to 5% in the trigonal (α) $ZrMo_2O_8$.

Fig. 7 shows the temporal evolution of the concentration (C/C_0) of MG, in which C_0 and C represent the initial equilibrium concentration and reaction concentration of MG, respectively. It can be seen that the sample prepared at 450°C shows a higher degree of photodegradation of MG (after 90 min irradiation time) as compared to the sample additionally calcinated at 600°C. Photoactivity of $ZrMo_2O_8$ obtained by us is compatible with that of $ZrMo_2O_8$ synthesized by Sahoo *et al.* using combustion method [15]. The better photocatalytic activity of $ZrMo_2O_8$ heated at 450°C is due to higher specific surface area as densification process is too low and there is no sintering of the particles (Fig. 3b). On the other hand according IR spectra the local microstructure (short-range order) is determined by the presence of deformed MoO_4 units. According to Sahoo *et al.* [15] this structural peculiarity is also a reason for higher degree of photocatalytical degradation. The photocatalytic test of both samples in the "dark" conditions without UV irradiation shown that $ZrMo_2O_8$ is not active.

4. Conclusions

The influence of heat-treatment on the phase and structural transformation of $ZrMo_2O_7(OH)_2$•$2(H_2O)$ has been investigated. It was established that the $ZrMo_2O_7(OH)_2$•$2H_2O$ was converted to orthorhombic LT-$ZrMo_2O_8$ at 200°C. The mixture of cubic and trigonal (α) $ZrMo_2O_8$ was obtained at 400°C. The higher photocatalytic activity of trigonal (α) $ZrMo_2O_8$ obtained at 450°C is related to its porous structure, higher specific surface area and the presence of distorted MoO_4 structural units.

5. Acknowledgments

This work was financially supported of the Bulgarian National Science Fund, Ministry of Education and Science Grants: TK-X-1718/07.

References

[1] P. Tarte, M. Auray, Solid State Chemistry, 3, 631 (1982)

[2] R.F. Klevtsova, L.A. Glinskaya, E.S. Zolotova, P.V. Klestsov, Dokl. Akad. Nauk. (SSSR) 3, 91 (1989) (In Russian)

[3] A.M.K. Andersen, S. Carlson, Acta Cryst. B57, 20 (2001)

[4] S. Carlson, A.M.K. Andersen, Phys. Rev. B61, 11209 (2000)

[5] S. Allen, R.J. Ward, M.R. Hampson, R.K.B. Gover, J.S.O. Evans, Acta Cryst. B60, 32 (2004)

[6] C. Lind, D.G VanDerveer, A.P. Wilkinson, J. Chen, M.T. Vaughan, D.J.Weider, Chem. Mater. 13, 487 (2001)

[7] C. Lind, A.P. Wilkinson, Z. Hu, S. Short, J.D. Jorgensen, Chem. Mater. 10, 2335 (1998)

[8] C. Lind, A.P. Wilkinson, C.J. Rawn, E.A. Payzant, J. Mater. Chem. 11, 3354 (2001)

[9] C. Lind, A.P. Wilkinson, J. Sol-Gel Sci. Technol. 25, 51 (2002)

[10] S. Allen, J.S.O. Evans, Phys. Rev. B 86, 134101 (2003)

[11] S. Allen, N.R. Warmingham, R.K.B. Gover, J.S.O. Evans, Chem. Mater. 15, 3406 (2003)

[12] G. Blasse, G.J. Dorksen, J. Phys. Chem. Solids. 48, 591 (1987)

[13] H. Liu, P. Cheung, E. Iglesia, J. Phys. Chem. B107, 4118 (2003)

[14] K. Chen, E. Iglesia, A.T. Bell, J. Phys. Chem. B105, 646 (2001)

[15] P. P. Sahoo, S. Sumithra, G. Madras, T.N.G. Row, J. Phys. Chem. C113, 10661 (2009)

[16] P. P. Sahoo, S. Sumithra, G. Madras, T.N.G. Row, Bull. Mater. Sci. 33, 337 (2009)

[17] A. Bojinova, R. Kralchevska, I. Poulios, C. Dushkin, Mater. Chem. Phys. 106, 187 (2007)

[18] N. Kaneva, G. Yordanov, C. Dushkin, Bull. Mater. Sci. 33, 11 (2010)

[19] G. Hunag, C. Zhang, Y. Zhu, J. Alloys and Comp. 432, 269 (2007)

[20] H.H. Li, K.W. Li, K. Wang, Mater. Chem. Phys. 116, 134 (2009).

[21] R. Iordanova, M. Mancheva, Y. Dimitriev, D. Klissurski, G. Tyuliev, B. Kunev, J. Alloys and Comp. 485, 104 (2009)

[22] R. Clearfield, H. Blessing, J. Inorg. Nucl. Chem. 34, 2643 (1972)

[23] D.V.S. Muthu, B. Chen, J.M. Wrobel, A.M.K. Andersen, S. Carlson, M.B. Kruger, Phys. Rev. B65, 64101 (2002)

[24] K. Nakamoto Infrared and Raman Spectra of Inorganic and Coordination, 5th edition (Wiley, New Work, 1997)

[25] J.S.O. Evans, T.A. Mary, T. Vogt, M.A. Subramanian, A.W. Sleight, Chem. Mater. 8, 2809 (1996)

[26] B. Chen, D.V.S. Muthu, Z.X. Liu, A.W. Sleight, M.B. Kruger, Phys. Rev. 64, 21411 (2001)

[27] K. Kanamori, T. Kineri, R. Fukuda, T. Kawano, K. Nishio, J. Mater. Sci. 44, 855 (2009)

[28] K.V.R. Chary, K.R. Reddy, G. Kishan, J.W. Niemantsverdriet, G. Mestl, J. Catal. 226, 283 (2004)

[29] S. Chang, R. Doong, Chem. Mater. 17, 4837 (2007)

[30] B.M. Reddy, B. Chowdhury, E.P. Reddy, A. Fernandez, J. Molec. Catal. A: Chem. 162, 431 (2000)

[31] A. Guerfi, R.W. Paynter, L.H. Dao, J. Electrochem. Soc. 142, 3457 (1995)

[32] F. Barath, M. Turki, V. Keller, G. Maire, J. Catal. 185, 1 (1999)

[33] F.P. Rouxinol, B.C. Trasferetti, R. Landers, M. A. Bica de Moraes, J. Braz. Chem. Soc. 15, 324 (2004)

[34] J. Torres, J.E. Alfonco, L.D. Lopez-Carreno, Phys. Stat. Sol (C). 10, 3726 (2005)

[35] J.Yu, L. Qi, B. Cheng, X. Zhao, J. Hazard. Mat. 160, 621 (2008)